Mode Selectivity in Bragg Reflection Waveguide Lasers

Cunzhu Tong, Bhavin J. Bijlani, L. J. Zhao, Sanaz Alali, Q. Han, and Amr S. Helmy

***Abstract*—Bragg reflection waveguides (BRWs) have recently been proposed for the development of high performance single mode lasers and nonlinear frequency conversion devices. In this letter, we experimentally demonstrate single transverse photonic bandgap mode operation in a large core BRW laser with low threshold current density ($\sim 594\ \mathrm{A/cm^2}$) and high characteristic temperature ($T_0 \sim 175$ K). The mode selectivity is examined theoretically using the effective index method and experimentally via far field and gain spectra measurements. Mode competition is found to take place among the lateral modes despite the optical thickness of the core layer being larger than the wavelength.**

***Index Terms*—Bragg reflection waveguides, mode selectivity, semiconductor lasers.**

I. Introduction

BRAGG reflection waveguide (BRW), essentially a one-dimensional (1-D) photonic bandgap (PBG) structure with a line-defect as the core layer, has been studied extensively in recent years [1]–[7]. This is due to their potential in applications related to nonlinear frequency conversion [2], [3]. Moreover, BRWs have also been predicted to enable the realization of high power lasers and amplifiers by providing laser cavities with single mode waveguides, with larger mode volumes [5], [6], higher gain coefficients [6] and stronger mode discrimination [5], [7], [8]. The aforementioned characteristics render BRWs as a promising platform to develop monolithically integrated optoelectronic integrated circuits (OEIC). Most notably electrically injected optical parametric oscillators and compact spontaneous parametric down conversion photon-pair sources can be achieved by integrating BRW lasers (BRLs) with nonlinear BRWs.

Manuscript received December 01, 2010; revised April 01, 2011; accepted April 15, 2011. Date of publication April 25, 2011; date of current version July 01, 2011. This work was supported by the Natural Sciences and Engineering Research Council of Canada (NSERC), by the Hundred Talents Program of the Chinese Academy of Sciences, and by the National Natural Science Foundation of China under Grant 61076064.

C. Tong is with the Edward S. Rogers Sr. Department of Electrical and Computer Engineering, University of Toronto, Toronto, ON, M5S3G4, Canada, and also with the Changchun Institute of Optics, Fine Mechanics and Physics, Chinese Academy of Sciences, Changchun, 130021, China (e-mail: cz.tong@utoronto.ca).

B. J. Bijlani, S. Alali, and A. S. Helmy are with the Edward S. Rogers Sr. Department of Electrical and Computer Engineering, University of Toronto, Toronto, ON, M5S3G4, Canada (e-mail: b.bijlani@utoronto.ca; Sanaz.alali@gmail.ca; a.helmy@utoronto.ca).

L. J. Zhao and Q. Han are with the Institute of Semiconductors, Chinese Academy of Sciences, Beijing, 100083, China (e-mail: ljzhao@semi.ac.cn; Hanqin@red.semi.ac.cn).

Color versions of one or more of the figures in this letter are available online at http://ieeexplore.ieee.org.

Digital Object Identifier 10.1109/LPT.2011.2147298

Recently, highly efficient nonlinear frequency conversion [3] and single mode lasing [4] have been achieved in BRWs. Theoretical studies were previously carried out examining the guided modes in the BRWs [6]–[8]. Systematic experimental and theoretical examination of the performance of this class of lasers was not previously presented. To explore the full potential of BRWs for high power laser applications, insight into their modal characteristics is necessary. In this Letter, we analyze the losses of guided modes in a ridge BRL structure using the effective index method (EIM) [9] and the transfer matrix method (TMM) [10]. Using this analysis, we verify the theoretical predictions of the mode discrimination in a BRL cavity. The mode selectivity is then experimentally investigated by examining the lasing spectra, the near and far field patterns, and the gain spectra.

II. Mode Losses in BRLs

The BRL structure is a ridge waveguide edge emitting diode laser. It consists of a low index core layer sandwiched between a top and a bottom Bragg reflectors [4]. The guided mode of this structure can be calculated using the EIM. In the calculations, we used the dimensions of the fabricated lasers. The structure consists of 8 pairs of top p-doped and bottom n-doped quarter-wave $Al_{0.3}GaAs_{0.7}As/GaAs$ Bragg stacks. Their thicknesses are 281 nm and 167 nm, respectively. The p- and n-doping concentrations in the reflectors are 5×10^{17} cm^{-3} and 1×10^{18} cm^{-3}, respectively. The gain medium consists of two 6 nm $In_{0.2}Ga_{0.8}As/GaAs$ quantum wells separated by 10 nm GaAs barriers. The operating wavelength is 980 nm. The core layer is 700 nm $Al_{0.37}Ga_{0.63}As$. From the scanning electron microscope (SEM) results, the ridge width, W, is 4.2 μm, the etch depth is 3.73 μm, and the cavity-length is 473 μm. This waveguide can be modeled as a symmetrical waveguide with a center region refractive index of n_{ey} and the side regions indices are n_{e1}. The corresponding effective refractive indices can be calculated using [9]:

$$W k_0 \sqrt{n_{ey}^2 - n_{eff}^2} = 2\tan^{-1}\left(\sqrt{\frac{n_{eff}^2 - n_{e1}^2}{n_{ey}^2 - n_{eff}^2}}\right) + p\pi, \quad (1)$$

where k_0 is the wave number, $p(= 0, 1, 2\ldots)$ is the mode number in the transverse direction. The refractive index n_{e1}, which is determined by the etch depth of the ridge and the local changes in the Fabry–Pérot resonance frequency [11], is about 2.14 for our devices. While n_{ey} is the effective index of the 1-D BRW and is given by [1]

$$n_{ey} = \sqrt{n_c^2 - \left[(2m+1)\frac{\lambda}{2d_c}\right]^2}\ (m = 0, 1, \ldots), \quad (2)$$

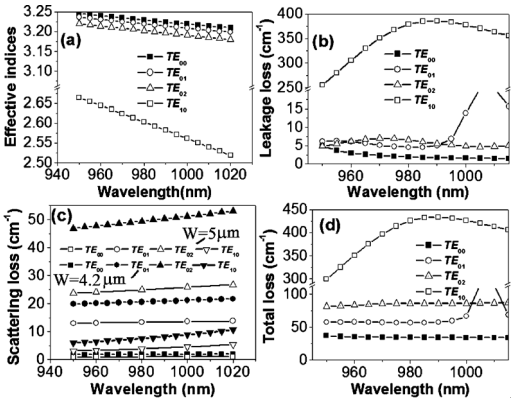

Fig. 1. Calculated (a) dispersion relation, (b) leakage loss, (c) scattering loss, and (d) total loss of guided TE_{00}, TE_{01}, TE_{02}, and TE_{10} modes in the 2-D ridge BRW.

where n_c and d_c are the refractive index and thickness of the core layer, λ is the free space wavelength, and m is the mode number in the growth direction. By substituting (2) into (1), we can get n_{eff} as a function of the mode numbers m and p. Fig. 1(a) shows the calculated effective indices of the transverse electric (TE_{mp}) modes in the BRL studied here. As can be seen, the modes TE_{0p} have nearly similar effective refractive indices, namely 3.23, 3.22 and 3.203 at 980 nm for TE_{00}, TE_{01} and TE_{02} modes, respectively. The corresponding dispersion coefficients of these modes, $dn_{eff}/d\lambda$, are -5.143×10^{-4} nm^{-1}, -5.429×10^{-4} nm^{-1} and -5.865×10^{-4} nm^{-1}. The higher order transverse mode TE_{10} shows a much lower effective index of 2.604 and dispersion of -2.086×10^{-3} nm^{-1}. The other high order transverse modes, such as $\mathrm{TE}_{2\mathrm{p}}$, are not guided in this waveguide due to the cut off condition of $m < (n_c d_c/\lambda - 1/2)$.

The leakage loss in a BRW due to the mode leakage in the growth direction can be expressed as [1]:

$$\alpha_L = \frac{-\lambda \ln |r|}{10 d_c^2 \mathrm{Re}(n_{eff})}. \tag{3}$$

Here, r is the reflectivity coefficient of Bragg reflectors and can be calculated by TMM [10]. Fig. 1(b) shows the calculated leakage losses of the TE_{mp} modes versus wavelength. It is clear that the higher order transverse mode, TE_{10}, shows much higher leakage loss than that of fundamental transverse modes (TE_{0p}). This result reflects the mode selectivity in BRWs. The leakage losses of TE_{0p} modes exhibit comparatively lower values $(< 5$ cm$^{-1})$ in the wavelength range between 970 nm and 1000 nm.

The loss of the ridge waveguide caused by scattering, can be expressed as [12]

$$\alpha_{s,p} = K^2 \frac{1}{2} \frac{\cos^3 \theta_p}{\sin \theta_p} \frac{1}{W}, \tag{4}$$

where, $K = \sigma_w(4\pi/\lambda)$, σ_w is the roughness of sidewall of ridge waveguide, and $\theta_p = \tan^{-1}\left\{\left[(n_{eff}^2 - n_{e1}^2)/(n_{ey}^2 - n_{eff}^2)\right]^{1/2}\right\}$. The scattering losses of TE_{mp} modes are plotted in Fig. 1(c). The value of σ_w was found to be ~ 300 nm from the topographic measurements of SEM. As shown in Fig. 1(c), the smaller the ridge-width and the higher the mode number p are, the higher the scattering losses becomes.

The free carrier absorption loss is also taken into account, and is ~ 5 and 7 cm^{-1} per 10^{18} cm^{-3} for n- and p-type AlGaAs [13], [14], respectively. The other part of the absorption loss can be obtained from the imaginary part of n_{eff}, which is ~ 2 cm^{-1} and 2.5 cm^{-1} for the TE_{0p} and TE_{1p} modes, respectively. Fig. 1(d) shows the sum of all the losses discussed above, as a function of wavelength. As can be seen, at the lasing wavelength of 980 nm, the loss of TE_{10} mode $(\sim 426.5$ cm$^{-1})$ is much higher than that of TE_{00} $(\sim 33.9$ cm$^{-1})$ and TE_{01} $(\sim 56.3$ cm$^{-1})$ modes. Hence, the most likely modes to lase, will be fundamental transverse modes TE_{0p}. This is a remarkable result given the optical thickness of the waveguide core is larger than the operating wavelength. For total internal reflection (TIR) based laser cavities, there are much more strict limitations on the waveguide core thickness to maintain single vertical transverse mode.

The BRLs were grown on 3°-off (100)-oriented, $n+$ GaAs substrate by metal-organic chemical vapor deposition (MOCVD). The details of the laser design were reported previously [4]. The samples were coated with 300 nm SiO_2, then 4 μm width ridges were defined by photolithography. The silica masks were formed by CHF_3 inductively coupled plasma (ICP) etching. After, the AlGaAs was etched using $BCl_3/Cl_2/Ar$ ICP. The dielectric etch mask was remove and a 300 nm SiO_2 isolation layer was deposited. An opening in the oxide layer was then patterned, where the top metal contact will take place. Contacts were deposited using e-beam evaporation. Samples were cleaved and mounted on copper heat-sinks without facet passivation or coating.

III. Results and Discussion

Fig. 2(a) shows the temperature dependent continuous- wave (CW) light–current $(L$–$I)$ curves. The maximum obtainable power from both facets is about 100 mW, while the highest slope efficiency is 0.465 W/A. The threshold current sensitivity to the temperature is 0.08 mA/°C, which leads to a characteristic temperature $T_0 \sim 175$ K in the range of 10–50°C. The lowest threshold current is 11.8 mA at 10°C, corresponding to a threshold current density of 594 A/cm^2. The polarization resolved power measurements (top inset in Fig. 2(a)) shows that $>95\%$ of the collected light is TE polarized. To examine the lasing modes, the lasing spectra were measured and shown in Fig. 2(b). As can be seen, the device operates in a single transverse mode up to 85 mA. Above 85 mA, a higher order mode appears at the wavelength of 984 nm. Upon increasing the injected current above 130 mA, we can observe another mode at the wavelength of 992 nm. These three modes persist until the thermal rollover of output power. The corresponding near-field patterns (NFP) are shown in Fig. 2(b). The discrete lobes demonstrate that the lasing is taking place in the PBG modes [4], which is further confirmed by the far-field results shown in Fig. 2(c). In contrast with TIR modes, the far-field distribution of the fundamental BRW mode is dual lobed with several symmetrical small peaks in the vertical direction.

The subthreshold emission spectrum (SES) shown in the bottom inset of Fig. 2(a) excludes the possibility that the lasing modes above 80 mA are the different longitudinal modes. As can be seen, there are nine peaks with almost similar wavelength separation (~ 7 nm) from 930 nm to 995 nm. A similar

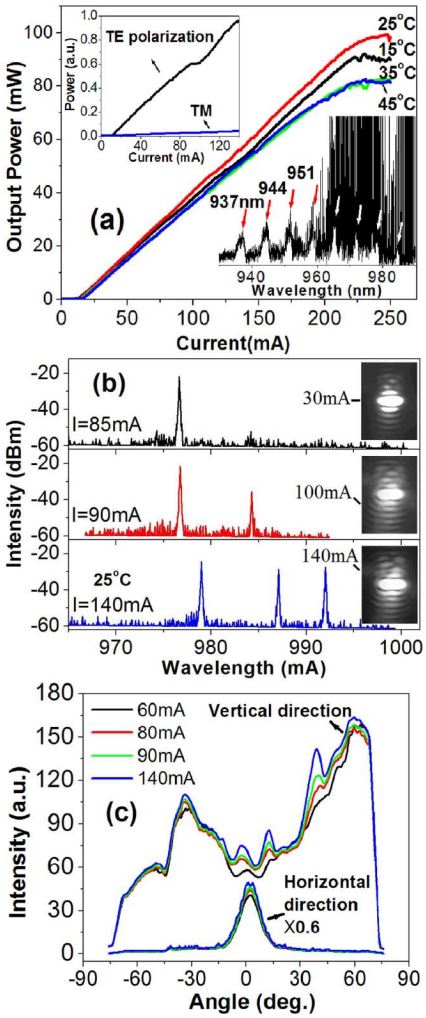

Fig. 2. Measured (a) CW L–I curves from 15 °C to 45 °C. The top inset shows the polarization discrimination; the bottom shows the SES. (b) Lasing spectra; (c) far-field profiles.

wavelength separation can also be observed in the lasing spectra shown in Fig. 2(b). These peaks do not correspond to the different longitudinal modes due to their large wavelength separation. According to the field distribution of BRW modes [1], [15], we can recognize that the first lasing mode (976 nm) is the fundamental mode, i.e., TE_{00} mode. The two lobes shown in the NFP measured at 100 mA confirm that the mode at 984 nm is the TE_{01} mode. The NFP measured at 140 mA is similar to that obtained at 100 mA. In other words, the lasing of mode 992 nm does not change the shape of NFP significantly. This suggests that the third lasing mode is likely to be TE_{02}, the reason being that the field distribution of the TE_{02} mode is similar to that of TE_{00} plus TE_{01} [15].

The net modal gains are gotten from SES using Hakki–Paoli method [16] and plotted in Fig. 3 for (a) TE_{00} and (b) TE_{01} mode. The further fits (solid lines) by the logarithmic relation $G = G_0 \ln(I/I_0) - \alpha$ show the modal losses independent from the cavity length, α, is 7.1 cm^{-1} and 34.6 cm^{-1} for TE_{00} and TE_{01} modes, respectively. The transparency current I_0 is 5.4 mA, which is same for all modes due to their same material gains. These results indicate that the threshold gains of TE_{00} and TE_{01} modes are 34.8 cm^{-1} and 62.3 cm^{-1}, respectively, which are in agreement with the calculated values shown in Fig. 1(d).

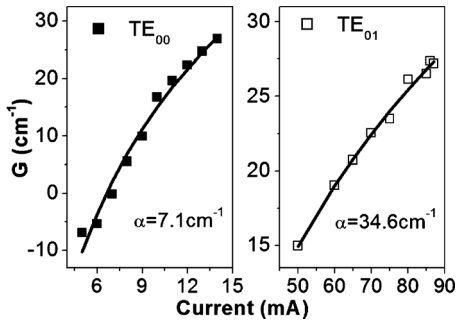

Fig. 3. Net gain of TE_{00} (solid squared) and TE_{01} (hollow squares) modes extracted from the SES.

IV. Conclusion

In summary, we have investigated the mode selectivity in the BRW ridge lasers. The single BRW PBG mode operation with low threshold current and high temperature stability is achieved. The quantitative modal loss/gain of TE_{00} and TE_{01} modes are measured, and shown to be consistent with the theoretical calculations. We believe these results will contribute to the performance improvement of the single mode operation of BRW PBG lasers.

References

[1] B. R. West and A. S. Helmy, "Properties of quarter wave Bragg reflection waveguides: Theory," *J. Opt. Soc. Amer. B*, vol. 23, pp. 1207–1220, 2006.

[2] A. S. Helmy, "Phase matching using Bragg reflection waveguides for monolithic non-linear applications," *Opt. Express*, vol. 14, pp. 1243–1252, 2006.

[3] P. Abolghasem, J. Han, B. J. Bijlani, and A. S. Helmy, "Type-0 second order nonlinear interaction in monolithic waveguides of isotropic semiconductors," *Opt. Express*, vol. 18, no. 19, pp. 12681–12689, 2010.

[4] B. Bijlani and A. S. Helmy, "Bragg reflection waveguide lasers," *Opt. Lett.*, vol. 34, pp. 3734–3736, 2009.

[5] A. Yariv, Y. Xu, and S. Mookherjea, "Transverse Bragg resonance laser amplifier," *Opt. Lett.*, vol. 28, pp. 176–178, 2003.

[6] L. Zhu, A. Scherer, and A. Yariv, "Modal gain analysis of transverse Bragg resonance waveguide lasers with and without transverse defects," *IEEE J. Quantum Electron.*, vol. 43, no. 10, pp. 934–940, Oct. 2007.

[7] J. Li and K. S. Chiang, "Guided modes of one-dimensional photonicbandgap waveguides," *J. Opt. Soc. Amer. B*, vol. 24, pp. 1942–1950, 2007.

[8] T. H. Her, "Gain-guiding in transverse grating waveguides for large modal area laser amplifiers," *Opt. Express*, vol. 16, pp. 7197–7202, 2008.

[9] K. Kawano and T. Kitoh, *Introduction to Optical Waveguide Analysis: Solving Maxwell's Equations and Schrödinger Equation*. Hoboken, NJ: Wiley Interscience, 2001.

[10] G. R. Hadley, "Effective index model for vertical-cavity surface-emitting lasers," *Opt. Lett.*, vol. 20, pp. 1483–1485, 1995.

[11] H. A. Macleod, *Thin-Film Optical Filters*. Bristol: Adam Hilger, 1986.

[12] P. K. Tien, "Light waves in thin films and integrated optics," *Appl. Opt.*, vol. 10, pp. 2395–2413, 1971.

[13] W. G. Spitzer and J. M. Whelan, "Infrared absorption and electron effective mass in n-type Gallium Arsenide," *Phys. Rev.*, vol. 114, pp. 59–63, 1959.

[14] D. I. Babic, J. Piprek, K. Streubel, R. P. Mirin, N. M. Margalit, D. E. Mars, J. E. Bowers, and E. L. Hu, "Design and analysis of double-fused 1.55-um vertical-cavity lasers," *IEEE J. Quantum Electron.*, vol. 33, no. 8, pp. 1369–1383, Aug. 1997.

[15] L. Zhu, X. Sun, G. A. De Rose, A. Scherer, and A. Yariv, "Spatial modal control of two-dimensional photonic crystal Bragg lasers," *Opt. Lett.*, vol. 32, pp. 2273–2275, 2007.

[16] B. W. Hakki and T. L. Paoli, "Gain spectra in GaAs double heterostructure injection lasers," *J. Appl. Phys.*, vol. 46, pp. 1299–1306, 1975.